


## Article

# Protein Kinase PoxMKK1 Regulates Plant-Polysaccharide-Degrading Enzyme Biosynthesis, Mycelial Growth and Conidiation in *Penicillium oxalicum*

Bo Ma , Xue-Mei Luo, Shuai Zhao \* and Jia-Xun Feng \*

State Key Laboratory for Conservation and Utilization of Subtropical Agro-Bioresources, Guangxi Research Center for Microbial and Enzyme Engineering Technology, College of Life Science and Technology, Guangxi University, Nanning 530004, China

\* Correspondence: shuaizhao0227@gxu.edu.cn (S.Z.); jiaxunfeng@sohu.com (J.-X.F.); Tel.: +86-771-3239401 (S.Z.)

**Abstract:** The ability to adapt to changing environmental conditions is crucial for living organisms, as it enables them to successfully compete in natural niches, a process which generally depends upon protein phosphorylation-mediated signaling transduction. In the present study, protein kinase PoxMKK1, an ortholog of mitogen-activated protein kinase kinase Ste7 in *Saccharomyces cerevisiae*, was identified and characterized in the filamentous fungus *Penicillium oxalicum*. Deletion of *PoxMKK1* in *P. oxalicum*  $\Delta$ *PoxKu70* led the fungus to lose 64.4–88.6% and 38.0–86.1% of its plant-polysaccharide-degrading enzyme (PPDE) production on day 4 after a shift under submerged- and solid-state fermentation, respectively, compared with the control strain  $\Delta$ *PoxKu70*. In addition, PoxMKK1 affected hypha growth and sporulation, though this was dependent on culture formats and carbon sources. Comparative transcriptomics and real-time quantitative reverse transcription PCR assay revealed that PoxMKK1 activated the expression of genes encoding major PPDEs, known regulatory genes (i.e., *PoxClrB* and *PoxCxrB*) and cellodextrin transporter genes (i.e., *PoxCdtD* and *PoxCdtC*), while it inhibited the essential conidiation-regulating genes, including *PoxBrlA*, *PoxAbaA* and *PoxFlbD*. Notably, regulons modulated by PoxMKK1 and its downstream mitogen-activated protein kinase PoxMKK1 co-shared 611 differential expression genes, including 29 PPDE genes, 23 regulatory genes, and 16 sugar-transporter genes. Collectively, these data broaden our insights into the diverse functions of Ste7-like protein kinase, especially regulation of PPDE biosynthesis, in filamentous fungi.

**Keywords:** *Penicillium oxalicum*; PoxMKK1; plant-polysaccharide-degrading enzyme; mycelial development



**Citation:** Ma, B.; Luo, X.-M.; Zhao, S.; Feng, J.-X. Protein Kinase PoxMKK1 Regulates Plant-Polysaccharide-Degrading Enzyme Biosynthesis, Mycelial Growth and Conidiation in *Penicillium oxalicum*. *J. Fungi* **2023**, *9*, 397. <https://doi.org/10.3390/jof9040397>

Academic Editor: Sotiris Amillis

Received: 14 February 2023

Revised: 17 March 2023

Accepted: 20 March 2023

Published: 23 March 2023



**Copyright:** © 2023 by the authors. Licensee MDPI, Basel, Switzerland. This article is an open access article distributed under the terms and conditions of the Creative Commons Attribution (CC BY) license (<https://creativecommons.org/licenses/by/4.0/>).

## 1. Introduction

Plant biomass is one of the most abundant and sustainable polymeric substrates used for the production of renewable bioenergy and commodity biochemicals, and it is comprised primarily of lignocellulose, which is rich in polysaccharides (such as cellulose and hemicellulose) and lignin (i.e., complex aromatic polymer) [1]. In the recent decades, the yields of renewable bio-based products from plant biomass-derived sugars have increased exponentially [2]. However, the often-inefficient saccharification of plant biomass still represents a key industrial bottleneck, largely resulting from its natural recalcitrance [3].

Fungi are widespread in a variety of natural environments and can exploit a wide range of carbon sources. They play a crucial role in the global carbon cycle because of their ability to break down plant biomass by secreting plant-polysaccharide-degrading enzyme (PPDE) [1,4]. Filamentous fungi are excellent producers of PPDE, where the expression of PPDE genes is finely regulated at both the transcriptional and post-translational levels [5]. Protein phosphorylation is the most common form of post-translational modification, functioning in many biological processes [6].

Many signals are transmitted by the mitogen-activated protein (MAP) kinase pathway, which is evolutionarily conserved and found ubiquitously from yeast to mammals [7]. The core elements of the MAP kinase (MAPK) pathway consist of three-tiered cascade kinases, termed MAPKKK (MAP kinase kinase kinase), MAPKK (MAP kinase kinase) and MAPK (MAP kinase), which are sequentially activated by a phosphorylation cascade, which is in turn initiated by the sensing of environmental stimuli using its upstream two-component signal transduction system or G-proteins-coupled receptors [7,8]. Five MAPK pathways have been identified in *Saccharomyces cerevisiae*, while only three of them have been found in many filamentous fungi [9].

The pheromone response/filamentation pathway, mediated by Ste11–Ste7–Fus3/Kss1, is the most extensively studied, and it is responsible for the regulation of fungal development, the production of secondary metabolites, and even pathogenicity in filamentous fungi [10]. However, it exhibits diversity in its regulatory functions in homologues and/or different components of the signaling pathways of filamentous fungus. For instance, deletion of the orthologous gene of yeast, *Ste11*, resulted in conidiation defects in *Cochliobolus heterostrophus* [11] but produced more spores in *Ashbya gossypii* [12]. The loss of *AbSte7* from *Alternaria brassicicola*, caused notably faster growth on potato dextrose agar (PDA) containing sorbitol [13], whereas a lack of Ste7-like kinase Mkk6 in *Beauveria bassiana* presented inconspicuous changes in sensitivity to sorbitol [14]. In *Ustilagoidea virens*, *UvPmk1* knockout demonstrated an increase in tolerance to cell wall stresses [15], while, conversely, *CcPmk1* deletion led to hypersensitivity to cell wall inhibitors in *Cytospora chrysosperma* [16]. Furthermore, in the plant pathogenic fungus *Colletotrichum gloeosporioides*, CgSte50, CgSte11, CgSte7, and CgMK1 were required for appressorium formation, penetration of the cellophane membrane, invasive growth, and pathogenicity, and also affected vegetative growth under nitrogen limitation conditions. Notably, CgSte50, CgSte11, and CgSte7, but not CgMk1, played important roles in the oxidative stress response [17]. However, the function of Ste7 homologues has not been investigated in detail in industrial filamentous fungus.

*Penicillium oxalicum* exhibits promise for application in ecological reconstruction, drug production, agricultural biocontrol, and biorefinery [18–20]. Meanwhile, as a fast-growing saprophytic fungus species, *P. oxalicum* can secrete various lignocellulolytic enzymes, and has potential for the production of industrial-scale PPDEs. Although many transcription factors (TFs) that regulate the expression of PPDE genes have been identified, few reports have been published regarding the signal transduction cascade in *P. oxalicum*. Heterotrimeric G protein, as an important component of the cell signaling cascade that transduces receptor signals to the intracellular environment, is involved in the regulation of PPDE production in *P. oxalicum*. For instance, G $\alpha$  subunit 3 mediates the G protein-cAMP signaling pathway in order to transduce various carbon source signals, and positively regulates the expression of TF-encoding gene *amyR*, subsequently affecting amylase and cellulase production [21]. The G $\gamma$  protein modulates PPDE production by mediating the expression of the regulatory gene *PoxCxrB*, a gene which is required for the expression of the major cellulase and xylanase genes. *PoxCxrB* also indirectly regulates the mRNA levels of major amylase genes by controlling the expression of *amyR* [22]. Recently, we found that the terminal component MAP kinase, *PoxMK1*, of the pathway positively regulated the expression of major PPDE genes and known essential regulatory genes—e.g., *PoxClrB* and *PoxCxrB*—in *P. oxalicum* [23].

In this work, *PoxMK1*-interacting proteins were screened by yeast-two hybrid assay (Y2H), and Ste7-homologous *PoxMkk1* (POX07948) was selected for further study. We characterized its roles in the regulation of PPDE production, vegetative growth and conidiation in *P. oxalicum* under both submerged (SmF) and solid-state (SSF) fermentation conditions, respectively.

## 2. Materials and Methods

### 2.1. Strains, Media and Growth Conditions

*P. oxalicum* HP7-1 (#10781; China General Microbiological Culture Collection, CGMCC), a wild-type strain isolated from the forest soil of Huaping National Natural Reserve in

Guilin, Guangxi, China, was reported previously [24]. In order to improve gene targeting frequency, *POX01583*, encoding the homologue of *Ku70* involved in the non-homologous end-joining pathway, was replaced in the wild-type HP7-1 by a hygromycin resistance gene via homologous recombination techniques [24]. The strain  $\Delta PoxKu70$  (#3.15650; CGMCC) was used as a background strain for the construction of deletion mutants, and then the mutant was used to construct the corresponding complementation strain. All *P. oxalicum* strains were maintained on potato dextrose agarose (PDA, Difco<sup>®</sup> Laboratories, Le Pont de Claix, Auvergne-Rhône-Alpes, France) for 6 days at 28 °C in order to collect asexual conidia through the use of sterile distilled H<sub>2</sub>O supplemented with 0.1% (*w/v*) Tween-80 (Sangon, Shanghai, China). The harvested spores were stored in 25% (*v/v*) glycerol at −80 °C for a long time.

For the determination of PPDE production, RNA sequencing, and real-time quantitative reverse transcription PCR (RT-qPCR), *P. oxalicum* conidia ( $1.0 \times 10^8$ ) were inoculated into 100 mL modified minimum medium [MMM, per liter: KH<sub>2</sub>PO<sub>4</sub> 4.0 g, (NH<sub>4</sub>)<sub>2</sub>SO<sub>4</sub> 4.0 g, MgSO<sub>4</sub>·7H<sub>2</sub>O 0.6 g, CaCl<sub>2</sub> 0.6 g, 1.0 mL Tween-80; FeSO<sub>4</sub>·7H<sub>2</sub>O 0.005 g, MnSO<sub>4</sub> 0.0016 g, ZnCl<sub>2</sub> 0.0017 g and CoCl<sub>2</sub> 0.002 g; pH 5.0] with 1.0% (*w/v*) D-glucose and cultivated for 24 h at 28 °C with shaking at 180 rpm [25]. Mycelia were harvested and transferred to MMM containing 2.0% Avicel (Avicel-PH101, Sigma-Aldrich, St. Louis, MO, USA), 1.0% soluble corn starch (SCS, Sigma-Aldrich, St. Louis, MO, USA) or wheat bran plus rice straw (WR), and the inoculated media were incubated for 2–4 days at 28 °C for enzyme activity measurement or for 4–48 h for RNA sequencing and RT-qPCR assay, respectively.

For assay of radial growth, five microliters of conidial suspension (approximately  $0.5 \times 10^5$  spores) were dropped onto solid plates containing PDA, complete medium [CM, per liter: 10.0 g D-glucose, 2.0 g peptone, 1.0 g yeast extract, 1.0 g acid-hydrolysed casein (Sangon, Shanghai, China), 6.0 g NaNO<sub>3</sub>, 0.52 g KCl, 0.52 g MgSO<sub>4</sub>·7H<sub>2</sub>O, 1.52 g KH<sub>2</sub>PO<sub>4</sub>; pH 6.5] and MMM containing 1.0% glucose, 1.0% SCS or 2.0% Avicel. The inoculated plates were incubated at 28 °C. For the evaluation of submerged growth, equivalent spores were inoculated in 100 mL liquid media of CM and MMM supplemented with 1.0 g glucose, 1.0 g SCS, and 2.0 g Avicel, respectively, and were then cultivated for 72 h at 28 °C with shaking at 180 rpm.

## 2.2. Yeast-Two Hybrid Assay

In order to construct plasmids for Y2H analysis, the full-length sequence of *PoxMK1* cDNA digested by the restriction enzymes *EcoRI* and *BamHI* was subcloned into the corresponding sites of pGBKT7 plasmid, as the bait, and the cDNA of candidate gene was subcloned into the *EcoRI* sites of pGADT7 plasmid, as the prey. All the cDNAs were amplified by PCR with special primer pairs (Supplementary Table S1), followed by verification through DNA sequencing. The verified bait plasmids were transformed into Y2H GOLD yeast-competent cells in order to test for toxicity and auto-activation activity on SD/-Trp plates using the lithium acetate/PEG protocol, and the bait and prey with candidate gene was co-transformed in to Y2H GOLD cells and placed on SD/-Leu/-Trp (DDO) plates. The transformant was verified by PCR amplification with special primer pairs (Supplementary Table S1) and then inoculated into liquid DDO medium cultivated for 1 day at 28 °C with shaking at 200 rpm. Ten microliters of tenfold serial dilution cells were grown on QDO plates with 150 mg/mL AbA and 20 ng/mL X- $\alpha$ -gal at 30 °C for 5 days. The experiment was performed twice independently.

## 2.3. Construction of Gene Deletion Mutant and Its Complementary Strain

For the generation of deletion mutant of each gene *POX04853*, *POX06496*, *POX07588*, and *POX07948*, the knockout cassette, containing 5' and 3' DNA fragments of the target gene and the G418-resistance gene fragment, was constructed by fusion PCR with specific primer pairs (Supplementary Table S1) according to previously published protocols [25]. Subsequently, the knockout cassette was directly transformed into fresh protoplasts of strain  $\Delta PoxKu70$ , the transformants were selected on G418-containing PDA plates, and then

knockout candidates were verified by PCR amplification using the special primer pairs (Supplementary Table S1). Similarly, the deletion mutant of *PoxMKK1* could also be obtained by the above method [23].

For the creation of a complementary strain of mutant  $\Delta POX07948$  ( $\Delta PoxMKK1$ )-, the complementary cassette was used to replace the protease gene *PoxPepA*, composed of the complete coding region of *PoxMKK1*, its native promoter and terminator, the bleomycin resistance gene fragment, and the upstream- and downstream-flanking DNA sequence of *PoxPepA*. The transformants were screened on PDA plate containing 80  $\mu\text{g}/\text{mL}$  bleomycin (Sigma-Aldrich, Darmstadt, Germany) and was validated by the special primer pairs (Supplementary Table S1), as previously described by Yan et al. [26].

#### 2.4. Molecular Manipulation

For total DNA extraction, *P. oxalicum* spores ( $\sim 10^8$ ) were transferred into liquid CM at 28 °C in a rotatory shaker (180 rpm) for 24 h. Subsequently, vegetative mycelia were collected through vacuum filtration and used for extraction of total DNA by following the modified phenol-chloroform method [24]. The genomic DNA was digested with *XhoI* (TaKaRa Bio Inc. Dalian, China) and separated from 0.75% agarose gel electrophoresis. Subsequently, the DNA was transferred onto the Hybond-N<sup>+</sup> nylon membranes (GE Healthcare Limited, Amersham, UK). Detection of the probe-hybridized DNA fragment was carried out using the DIG High Prime DNA Labeling and Detection Starter Kit I following the manufacturer's protocol (Roche Diagnostics, Mannheim, Germany). The probe was amplified by special primers sPOX07948-F/sPOX07948-R for Southern hybridization (Supplementary Table S1).

For total RNA extraction, mycelia were harvested and separated by filtering the culture with an eight-layer filter fabric, after which they were washed three times using diethyl pyrocarbonate-treated water prior to RNA extraction. Total RNA isolation was performed using Trizol reagent (Invitrogen, Carlsbad, CA, USA) according to the manufacturer's instructions.

#### 2.5. RNA Sequencing and RT-qPCR Analysis

For RNA sequencing, total RNA was extracted from the mycelia of *P. oxalicum* strains ( $\Delta PoxMKK1$  and  $\Delta PoxKu70$ ) exposed on Avicel for 24 h, treated with DNase I and purified after mRNA enrichment using oligo (dT) according to the manufacturer's guidelines. mRNA sequencing was carried out on a BGISEQ-500 platform at BGI (Shenzhen, China). The sequenced data were processed as described by Yan et al. [26]. Values in terms of Fragments per kilobase of exon per million mapped reads (FPKM) represented gene transcriptional levels, and differentially expressed genes (DEGs) were screened with a standard of probability  $\geq 0.8$  and  $|\log_2(\Delta PoxMKK1\_FPKM/\Delta PoxKu70\_FPKM)| \geq 1$ . Similarly, DEGs between  $\Delta PoxMKK1$  and  $\Delta PoxKu70$  were also selected with the same standard and were described in detail in Reference [23].

For comprehensive deciphering of the transcription profiling of  $\Delta PoxMKK1$  in response to Avicel, the DEGs were annotated according to the gene ontology (GO) knowledge base. DEGs were enriched and functionally classified by Blast2GO program with Fisher's exact test in association with a false discovery rate (FDR) correction for multiple testing ( $FDR < 0.05$ ) [27].

The RT-qPCR assay was conducted on an ABI 7500 Real-System (Thermo Fisher Scientific, Waltham, MA, USA). The Bio-Rad iQ5 software was used to compile PCR protocols and to define the plate setup. The PCR reaction mixture and program were referred to in the previous report [23]. The primer sequences used were listed in Supplementary Table S1. LightCycler480 software 1.5.0 was used to calculate the Ct value. The transcription levels of target genes were normalized against the level of actin gene (*POX09248*), as the endogenous reference gene, with  $2^{-\Delta\Delta Ct}$  relative quantification method [28]. All samples were analyzed in three independent experiments with three replicates.



### 2.6. Determination of Enzyme Activity and Protein Concentration

The preparation of crude enzyme solution and the determination of PPDE activities were implemented as previously described [26,29]. For crude enzyme solution preparation under SmF conditions, the culture was centrifuged at  $11,300\times g$  for 10 min at 4 °C, and the supernatant was stored at 4 °C for further analysis of enzyme activity. Under SSF conditions, the cultivated solid medium was added to 200 mL sterile ddH<sub>2</sub>O and crushed by a glass rod, then the mixture was shaken at 180 rpm for 2 h at 28 °C before being squeezed and centrifuged at  $11,300\times g$  for 20 min. The supernatant was used as a crude enzyme solution.

In order to measure PPDE activity, filter paper cellulase (FPase), carboxy methyl cellulase (CMCase), soluble starch-degrading enzyme (SSDE), raw starch-degrading enzyme (RSDE) and xylanase were assayed against Whatman No. 1 filter paper (1.0 cm  $\times$  6.0 cm; GE Healthcare Limited, Little Chalfont, Buckinghamshire, UK), CMC-Na (Sigma-Aldrich, Darmstadt, Germany), SCS (Sigma-Aldrich, Darmstadt, Germany), raw cassava starch (self-preparation) and xylan from beechwood (Megazyme International Ireland, Wicklow, Ireland) using a DNS method, respectively. The activities of *p*-nitrophenyl- $\beta$ -cellobiosidase (pNPCase) and *p*-nitrophenyl- $\beta$ -glucopyranosidase (pNPGase) were evaluated against *p*-nitrophenyl- $\beta$ -D-cellobioside (pNPC) and *p*-nitrophenyl- $\beta$ -D-glucopyranoside (pNPG) (Sigma-Aldrich, Darmstadt, Germany), respectively. The activity unit (U) was defined as the amount of enzyme required to produce one mol of reducing sugar or *p*-nitrophenyl per minute from the reaction substrates.

In addition, the protein concentration of mycelia cells was determined using the Detergent Compatible Bradford Assay Kit (Pierce Biotechnology, Rockford, IL, USA) against a BSA standard.

### 2.7. Phenotypic and Growth Analyses

For radial growth assay, the diameters of colonies found on different media cultured for 5 days were determined through two measurements taken perpendicular to each other across the center as indices of radial growth rates, and a Canon EOS 600D (Canon, Japan) was used for photography. For liquid growth assay, mycelia were collected by vacuum filtration at 12 h intervals in liquid CM and MMM with 1.0% (*w/v*) glucose or SCS and were then washed three times with deionized water. The mycelia were dried at 50 °C to a constant weight. However, the growth was indirectly measured by the amount of intracellular protein in liquid MMM with 2.0% (*w/v*) Avicel, as described above. All of the tests were repeated three times. Furthermore, the hypha of *P. oxalicum* in liquid medium were observed on day 2 after inoculation under a light microscope (OLYMPUS DP480, Olympus, Tokyo, Japan), and the photomicrographs were taken and analyzed by Olympus cellSens Dimension digital imaging software (Version 1.14).

### 2.8. Quantification of Conidia Production

In order to investigate the effect of PoxMKK1 on conidiation in *P. oxalicum*, the spores were counted using a hemocytometer on solid plates and in liquid culture, respectively. In the case of spores on solid plate, conidia were washed twice by 5.0 mL sterile ddH<sub>2</sub>O with 0.1% Tween-80, and the conidial suspension was mixed thoroughly and filtered through two layers of sterile gauze. Subsequently, the collected conidia were washed and ultimately re-suspended in ddH<sub>2</sub>O. The conidia production was quantified with the number of conidia per unit of colony area. For spores in the liquid culture, the culture was filtered through sterile gauze in order to remove the hyphae and medium residues, and the collected filtrate was diluted appropriately and used for conidia counting. Conidia production was indicated by the number of conidia per milliliter. Three biological replicates were performed for each strain.

### 2.9. Protein Sequence Analysis

The Simple Modular Architecture Research Tool (SMART, <http://smart.emblheidelberg.de/> (accessed on 6 July 2020)) and InterPro online (<http://www.ebi.ac.uk/interpro/> (ac-

cessed on 8 July 2020)) were used for prediction of the conserved domains contained in the PoxMKK1. The homologous sequences of MAP kinases from different fungi were searched with BlastP and downloaded from GenBank. Multiple sequence alignment was carried out using ClustalX 2.0 [30], and the phylogenetic tree was constructed by MEGA-X using the neighbor-joining method [31].

#### 2.10. Accession Numbers

The transcriptomic data of the *P. oxalicum* strains have been loaded into the Sequence Read Archive database (accession No. GSE154710). In addition, the sequence of PoxMKK1 was submitted to GenBank with accession number MT468562.

### 3. Results

#### 3.1. POX07948 Interacting with PoxMKK1 Is Required for FPase Production in *P. oxalicum*

A previous work found that MAP kinase PoxMK1 modulated the production of PPDE in *P. oxalicum* under both SmF and SSF conditions. Here, the Y2H was used to screen for PoxMK1-interacting proteins in *P. oxalicum*. The full-length PoxMK1 was used as bait, and the differentially phosphorylated TFs and kinases reported previously as a result of *PoxMK1* deletion [23] were used as prey. A total of four PoxMK1-interacting proteins (POX04853, POX06496, POX07588, and POX07948) were identified (Supplementary Figure S1).

In order to test whether these identified PoxMK1-interacting proteins were involved in the cellulase production of *P. oxalicum*, all of them were deleted in the control strain  $\Delta PoxKu70$  in order to generate the corresponding mutants  $\Delta POX04853$ ,  $\Delta POX06496$ ,  $\Delta POX07588$ , and  $\Delta POX07948$ , which were validated by PCR (Supplementary Figure S2A) with specific primers (Supplementary Table S1). When cultured in MMM containing 2.0% Avicel as the sole carbon source for 2–4 days after a shift from glucose, mutant  $\Delta POX06496$  showed 32.3–55.0% increased FPase production as compared with the  $\Delta PoxKu70$ , whereas mutant  $\Delta POX07948$  lost 41.2–92.9% of its FPase production. In contrast, mutants  $\Delta POX04853$  and  $\Delta POX07588$  exhibited similar FPase production to  $\Delta PoxKu70$  (Supplementary Figure S3). These data displayed that POX07948 positively participated in the regulation of cellulase production, and it was therefore selected for further study.

Southern hybridization analysis was performed with a special probe (Supplementary Table S1) in order to further determine whether the single copy of the *POX07948* deletion cassette was integrated into the right site of the  $\Delta PoxKu70$  genome (Supplementary Figure S2B). The complementary strain *CPOX07948* was generated by introducing the complementary cassette to deletion mutant  $\Delta POX07948$  as described previously [26], and the bleomycin-resistant transformants were isolated and verified by PCR with special primers (Supplementary Table S1). The expected size bands were amplified, as shown in Supplementary Figure S4.

#### 3.2. Characterization and Phylogenetic Analyses of PoxMKK1 in *P. oxalicum*

The POX07948 protein was composed of 557 amino acids, encoded by gene *POX07948* with a length of 1925 bp, containing three introns, according to the genome annotation of *P. oxalicum* strain HP7-1 [20]. The Simple Modular Architecture Research Tool (SMART) and InterPro online analyses indicated that the POX07948 protein contained a conserved serine/threonine protein kinase catalytic (S\_TKc) domain from residues 67–333, whose ATP-binding region and protein kinase activity site were located at residues 73–96 and 186–198, respectively (Figure 1A). An NCBI BlastP search revealed that the POX07948 protein shared 100%, 78.30%, 67.66%, and 44.33% of its identity with its homologous proteins from *P. oxalicum* 114-2 (GenBank accession No. EPS26612), *Aspergillus fumigatus* Af293 (EAL92976), *Talaromyces amestolkiae* CIB (RAO73071), and *S. cerevisiae* S228C (DAA11702), respectively. Moreover, phylogenetic analysis showed that the POX07948 protein was resolved in the Ste7 clade and visibly separated from the Pbs2 and Mkk1/2 clades (Figure 1B). In order to handily study further, POX07948 was denominated as PoxMKK1.

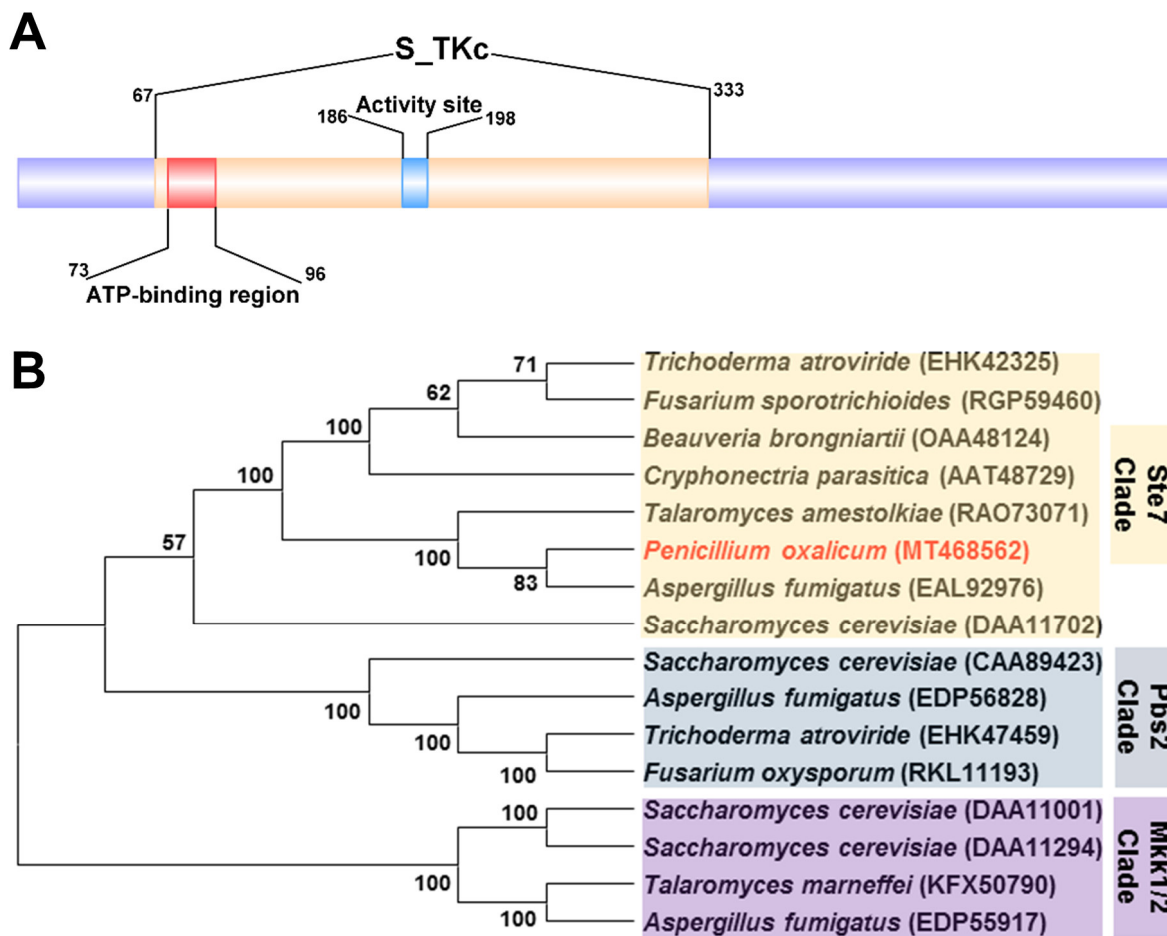


**Figure 1.** Structure and phylogenetic analyses of protein kinase PoxMKK1 (POX07948). (A) Conserved domain. S\_TKc, serine/threonine protein kinase catalytic domain. (B) Phylogenetic tree of PoxMKK1 and its homologs. The phylogenetic tree was generated by the MEGA X software using the neighbor-joining (N-J) method. The numbers at the branch nodes are bootstrap values (>50%) based on 1000 replicates.

### 3.3. PoxMKK1 Is Involved in Mycelial Growth and Conidiation in *P. oxalicum*

In order to examine the effects of *PoxMKK1* deletion on the vegetative growth and sporulation of *P. oxalicum*, the colony diameter and hypha biomass, as well as the spore number, were measured on solid or liquid medium, respectively. Fresh spores ( $0.5 \times 10^6$ ) of the mutant  $\Delta PoxMKK1$ , control strain  $\Delta PoxKu70$ , and complementary strain *CPoxMKK1* were directly pointed on PDA and MMM plates containing distinct carbon sources cultivated for 4 days at 28 °C. Compared with the control strain  $\Delta PoxKu70$  and complementary strain *CPoxMKK1*, the colony diameter of mutant  $\Delta PoxMKK1$  became larger on PDA ( $p < 0.01$ , Student's *t*-test), but not on glucose, SCS, or Avicel (Figure 2A,B). Furthermore, the colony color of  $\Delta PoxKu70$  and *CPoxMKK1* on PDA plates was black-brown, while that of the  $\Delta PoxMKK1$  mutant was black-green (Figure 2A). Notably, the colony center color of  $\Delta PoxKu70$  and *CPoxMKK1* was pale green on MMM containing Avicel, while that of the  $\Delta PoxMKK1$  mutant was grey, which might have resulted from different numbers of spores. Therefore, the spore number was quantified, and the result showed that the conidial production of  $\Delta PoxMKK1$  was significantly less than that of the control and complementary strains on PDA, glucose, SCS, and Avicel cultivated for 5, 14, 14, and 7 days, respectively (Figure 2C).

For samples grown under liquid culture conditions, the mycelium dry weight or intracellular protein were measured in MMM supplied with glucose, SCS, or Avicel, and CM. Surprisingly, the mycelial biomass of mutant  $\Delta PoxMKK1$  had no significant difference relative to that of  $\Delta PoxKu70$  when cultivated in MMM containing SCS or CM (Supplemen-

tary Figure S5A,B), whereas the growth of  $\Delta PoxMKK1$  mutant decreased during the whole cultivation stage in MMM with either glucose or Avicel (Supplementary Figure S5C,D). In addition, the asexual spore yields of  $\Delta PoxMKK1$  increased notably compared to those of  $\Delta PoxKu70$  and  $CPoxMKK1$  in the aforementioned liquid media when grown for 6 days at 28 °C with shaking at 180 rpm (Supplementary Figure S6). Moreover, microscopic observation showed that there were a number of phialides for conidiation at the top segments of the hyphae in the  $\Delta PoxMKK1$  mutant when cultivated on glucose, Avicel, or SCS for two days, whereas these were absent in both  $\Delta PoxKu70$  and  $CPoxMKK1$  (Figure 3), suggesting that *PoxMKK1* repressed mycelial development. Collectively, these findings indicated that *PoxMKK1* was involved in vegetative growth and conidiation which was dependent on culture formats and media.

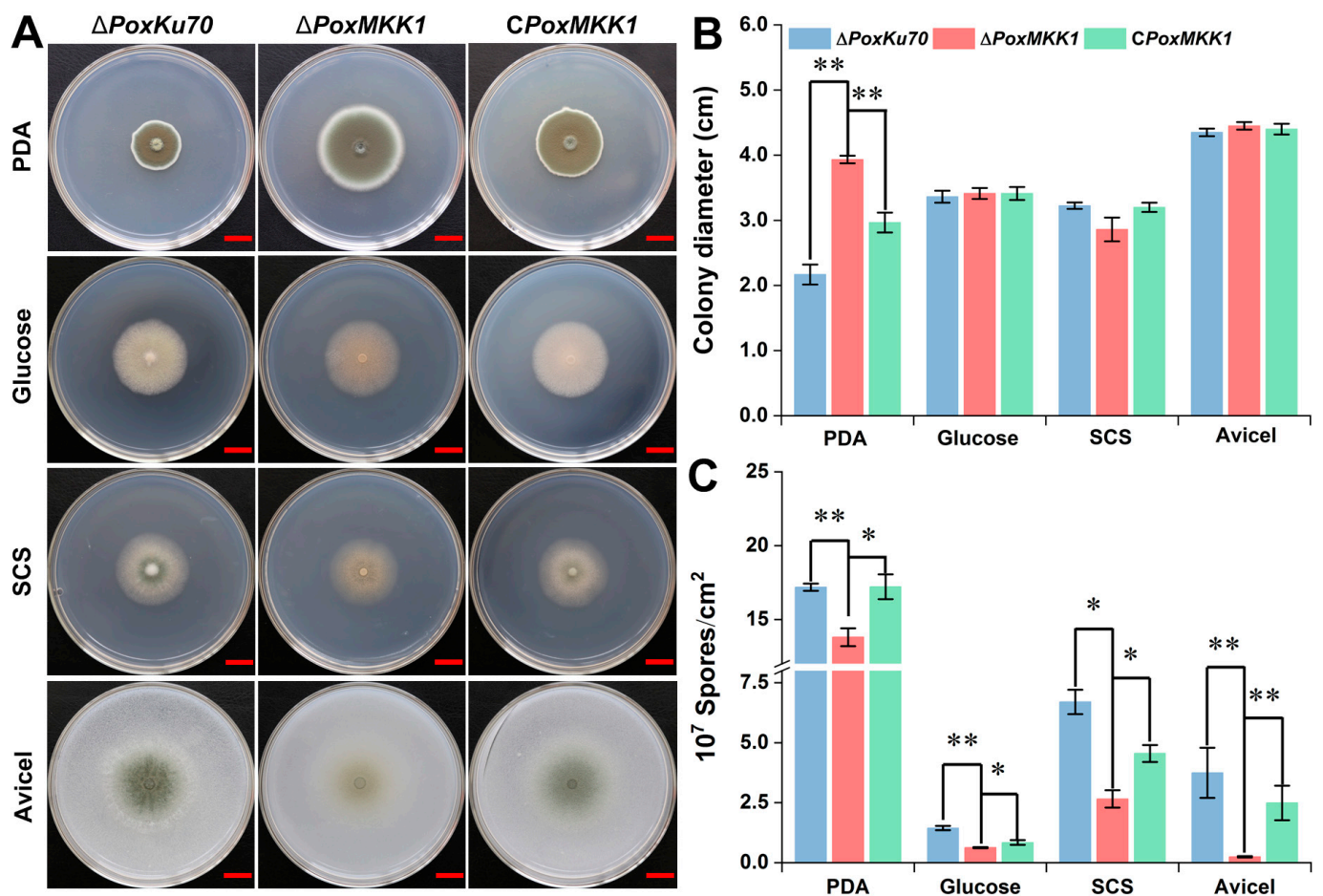


**Figure 2.** Phenotype characteristics of *P. oxalicum* mutant  $\Delta PoxMKK1$ , the control strain  $\Delta PoxKu70$ , and complementary strain  $CPoxMKK1$  on the different solid plates. (A) Colony morphology grown for 4 days. Scale bars = 1.0 cm. (B) Colony diameter. (C) Spore count. The number of spores was counted on PDA at 28 °C for 5 days, on MMM with 1.0% glucose and 1.0% SCS for 14 days, and on 2.0% Avicel for 7 days, respectively. PDA, potato dextrose agarose. MMM, modified minimum medium. SCS, soluble corn starch. The symbols \* and \*\* showed significant differences (\*  $p < 0.05$ , \*\*  $p < 0.01$ ) between mutant  $\Delta PoxMKK1$  and the control strain  $\Delta PoxKu70$ , and between mutant  $\Delta PoxMKK1$  and complementary strain  $CPoxMKK1$ , as assessed by Student's *t*-test.

### 3.4. Loss of *PoxMKK1* Alters PPDE Production of *P. oxalicum* under SmF and SSF

In order to further confirm the effects of *PoxMKK1* deletion on PPDE production in *P. oxalicum*, the mutant  $\Delta PoxMKK1$  and control strain  $\Delta PoxKu70$  were individually cultivated for 2–4 days after a shift from glucose, and their secreted PPDE productions were monitored. As depicted in Figure 4, when grown on Avicel under SmF for 2–4 days, the  $\Delta PoxMKK1$



displayed decreased FPase, CMCase, pNPCase, and xylanase production by 24.6–68.3%, as compared with that in  $\Delta PoxKu70$  ( $p < 0.05$ , Student's *t*-test). Notably,  $\Delta PoxMKK1$  showed a 2.6-fold increase in pNPGase production on day 2 and an 88.6% decrease on day 4 (Figure 4D). When cultivated on SCS under SmF for 4 days, both the RSDE and SSDE of the  $\Delta PoxMKK1$  were reduced by 64.4% and 64.8%, respectively (Figure 4F,G). Interestingly, the yields of cellulase and xylanase by the  $\Delta PoxMKK1$  were also depressed on WR under SSF by 37.4–93.2% and 26.0–57.2%, respectively (Figure 4H–L). As expected, the production of cellulase, xylanase, and amylase by the complementation strain  $CPoxMKK1$  was restored to the level of that by the  $\Delta PoxKu70$  cultivated as described above ( $p < 0.05$ , Figure 4).

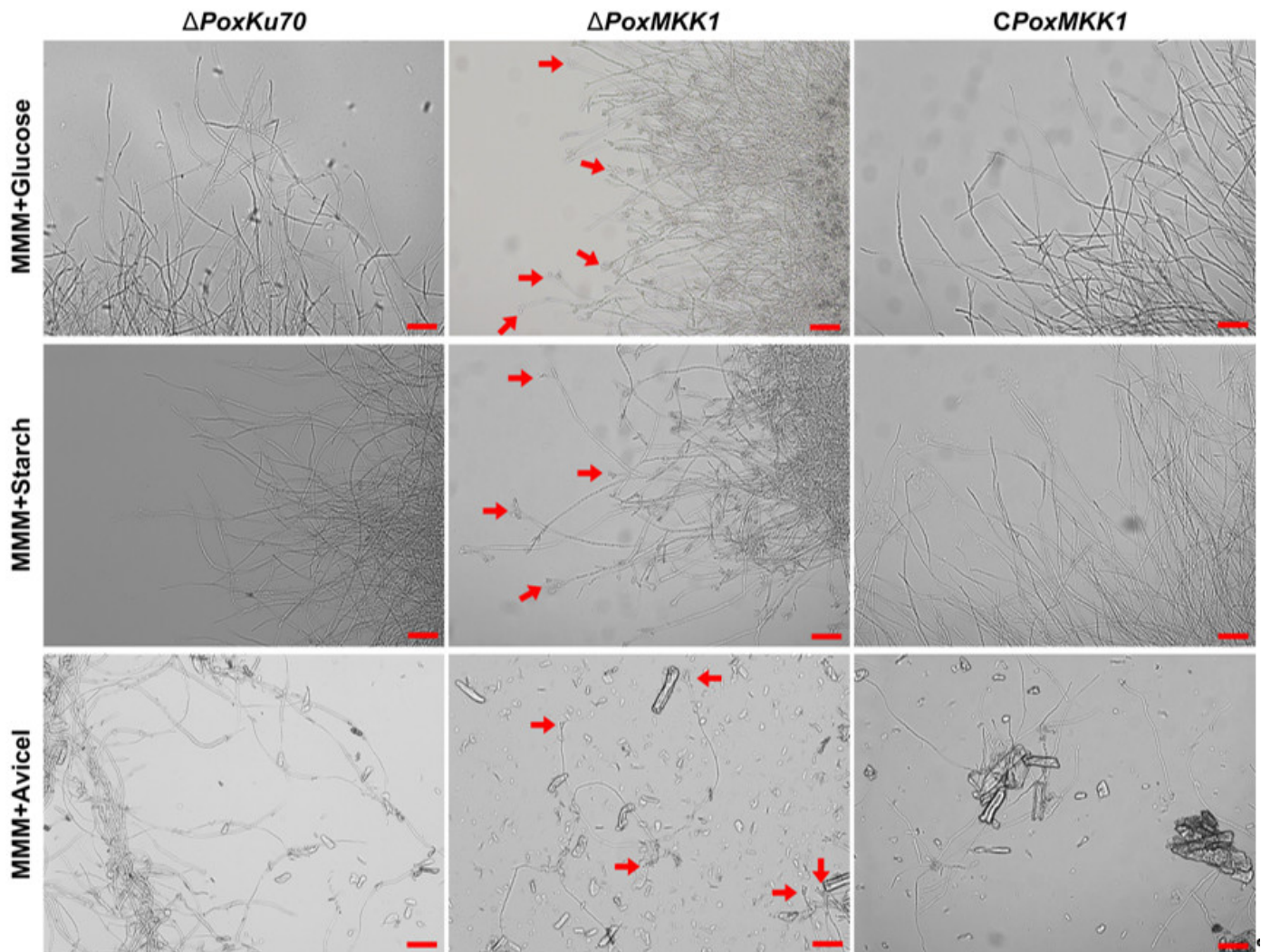


**Figure 3.** Microscopic images of hyphae in MMM containing 1.0% glucose, 1.0% SCS, and 2.0% Avicel as the solo carbon source at 28 °C for 24 h with 180 rpm ( $10^8$  conidia/mL). The red arrowheads point to conidiophores. Scale bars = 50  $\mu$ m.

### 3.5. RNA-seq Analyses Revealed the Global Regulation of *PoxMKK1* in *P. oxalicum*

In order to elucidate the functions of *PoxMKK1* on genome-scale gene expression in *P. oxalicum*, the mutant  $\Delta PoxMKK1$  and control strain  $\Delta PoxKu70$  were first grown in glucose medium for 24 h, and then the mycelia were transferred to Avicel medium for 24 h. The samples were used to isolate total RNA and for sequencing. As displayed in Supplementary Figure S7, a good Pearson's correlation coefficient was obtained ( $R > 0.92$ ) among the three biological repeats for each strain. The generated data displayed that more than 98% of the clean reads of  $\Delta PoxKu70$  and  $\Delta PoxMKK1$  were successfully aligned to the *P. oxalicum* HP7-1 genome [20]. With the criteria of probability  $\geq 0.8$  and

$|\text{Log}_2(\Delta PoxMKK1\_FRKM/\Delta PoxKu70\_FRKM)| \geq 1.0$ , a total of 1114 differential expression genes (DEGs) were selected in mutant  $\Delta PoxMKK1$ , relative to the control strain  $\Delta PoxKu70$ , including 634 upregulated and 480 downregulated genes (Supplementary Table S2).

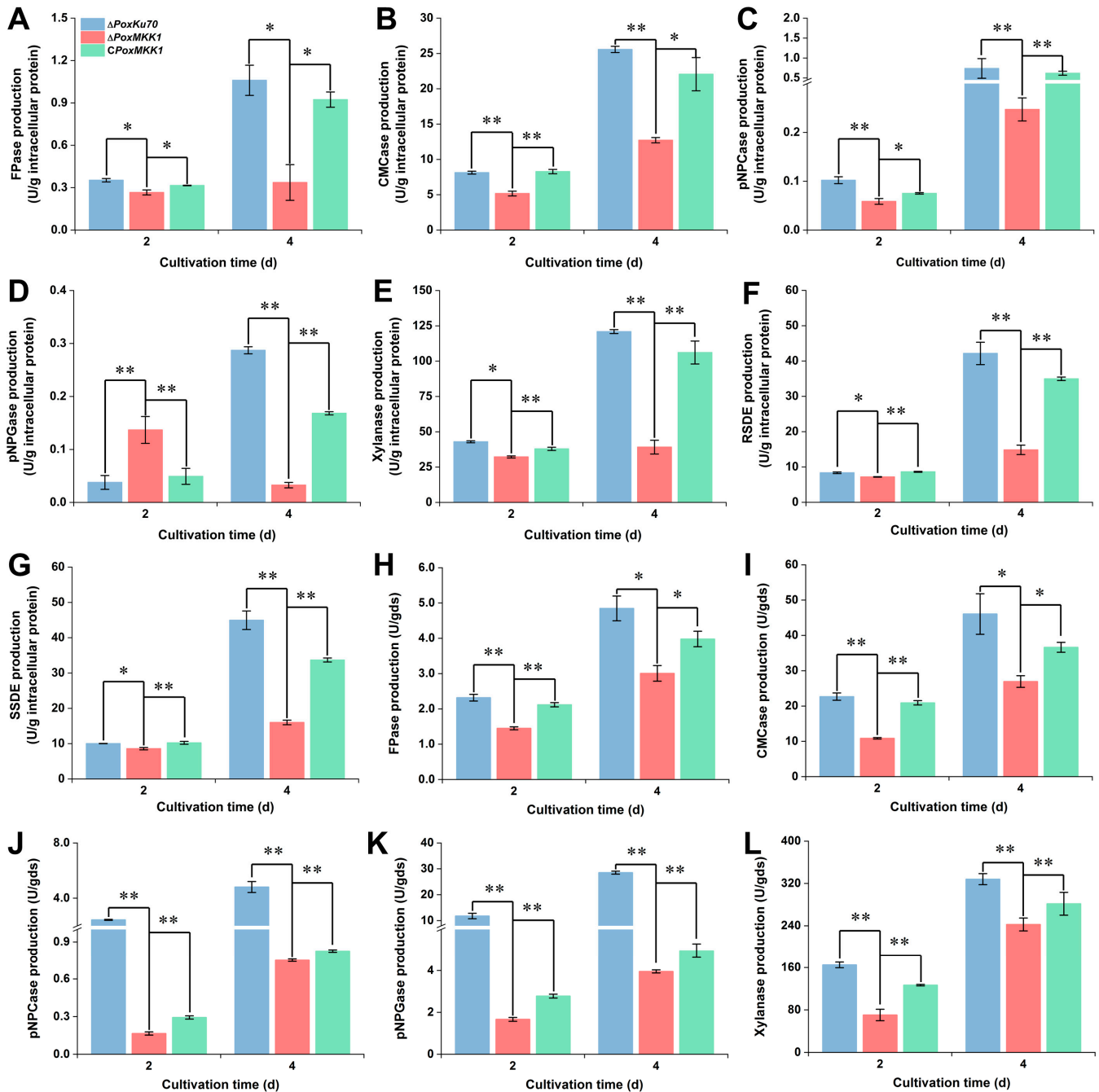


**Figure 4.** Protein kinase PoxMKK1 affects PPDE production in *P. oxalicum*. Cellulase (A–D,H–K) and xylanase (E,L) production are determined in liquid medium with 2.0% Avicel and solid medium containing wheat bran plus rice straw under SmF and SSF, respectively. (F) RSDE and (G) RSDE. Production was performed in liquid medium with 1.0% SCS. Enzymatic activity was assayed at 2–4 days after a shift from glucose. SSDE, soluble starch-degrading enzyme. RSDE, raw cassava starch-degrading enzyme. SmF, submerged fermentation. SSF, solid-state fermentation. Error bars indicate standard deviations of these results from three biological replicates. Significant differences are indicated by an asterisk between the deletion mutant  $\Delta PoxMKK1$  and the control strain or the complementation strain  $CPoxMKK1$ , respectively (\*  $p < 0.05$ , \*\*  $p < 0.01$ , Student's  $t$ -test).

GO enrichment analyses implied that 15 of the top 20 enriched terms were associated with molecular function, such as hydrolase activity (GO: 0016798 and GO: 0004553), catalytic activity (GO: 0003824), and carbohydrate binding (GO: 0030246, GO: 0030247, and GO: 0030247). Additionally, the DEGs in the  $\Delta PoxMkk1$ , which participated in the carbohydrate metabolic process and encoded extracellular region components, were also significantly enriched (Figure 5A).

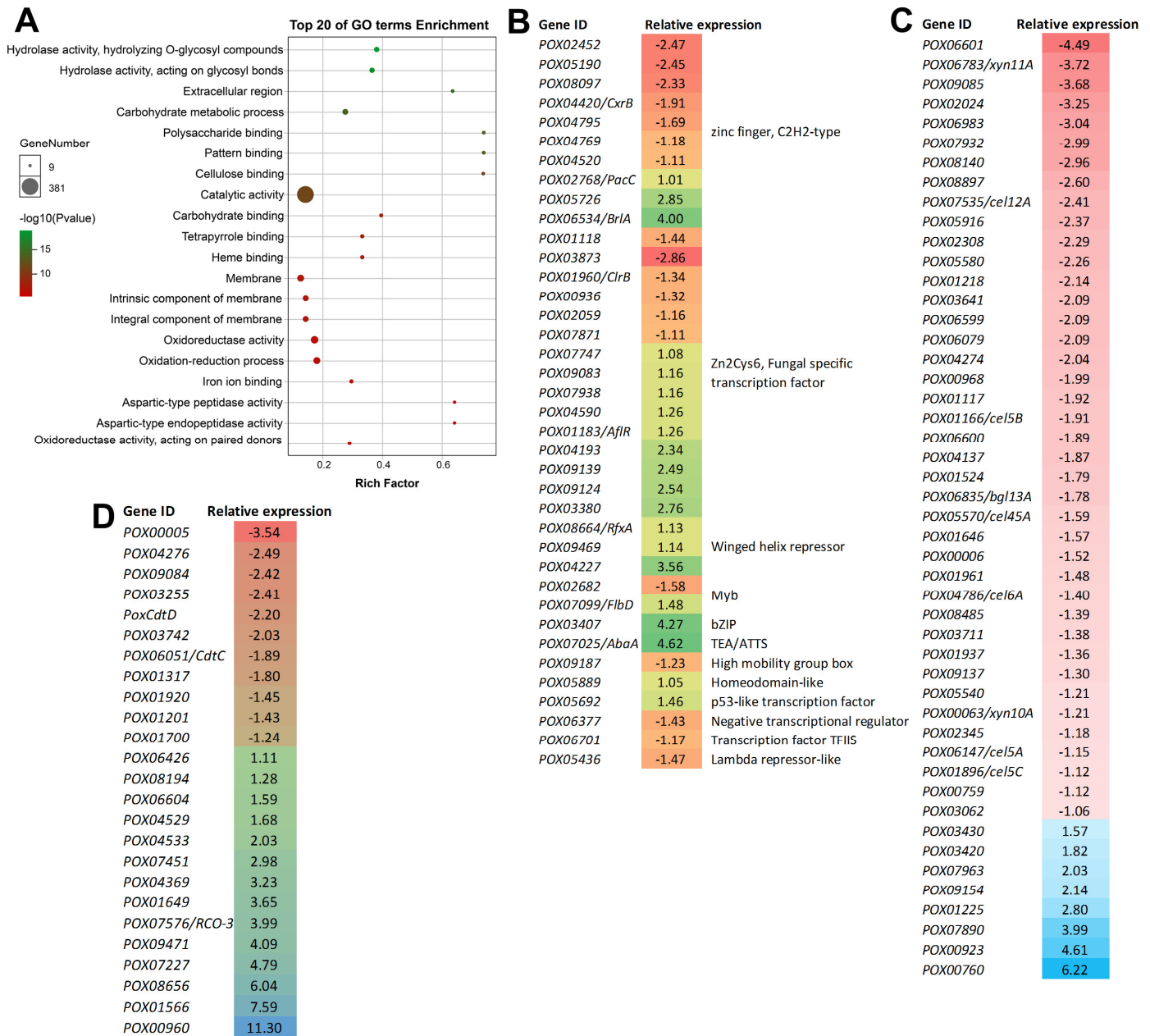


**Figure 5.** Transcriptomic analysis of the *P. oxalicum* mutant  $\Delta PoxMkk1$  and the control strain  $\Delta PoxKu70$  grown in MMM with 2.0% Avicel. Total RNAs for RNA sequencing were prepared from fungal hypha cultivated for 24 h after a shift. (A) The gene ontology (GO) annotation of differentially expressed genes (DEGs) for the top 20 GO terms' enrichment. (B–D) Heatmap showing the transcription abundance of DEGs encoding putative CAZymes, transcription factors (TFs), and sugar transporters. FPKM, fragments per kilobase of exon per million mapped reads.

Remarkably, of the 1114 DEGs, there were 133 genes encoding carbohydrate-active enzymes (CAZymes), including 48 plant cell-wall degrading enzymes (CWDEs). Of them, 40 DEGs were downregulated by 52.19–95.53% in mutant  $\Delta PoxMKK1$ , such as one CBH gene (*cbh2*), seven EG genes (*Cel5B*, *Cel45A*, *Cel5A*, *eg2*, *Cel5C*, *POX04137*, and *POX06983*), five BGL genes (*Bgl1*, *POX00923*, *POX00968*, *POX03062*, and *POX03641*), five xylanase genes (*Xyn10A*, *Xyn11A*, *POX04274*, *POX06601*, and *POX05916*), two lytic polysaccharide monoxygenases genes (*AA9A* and *POX02308*), and two expansin-like protein genes (*POX01524* and *POX08485*) (Figure 5B).

Besides CAZyme-encoding genes, the DEGs also contained 38 TF-encoding genes (Figure 5C). Among them, 18 DEGs were downregulated ( $-2.86 < \log_2$  (fold change)  $< -1.11$ ) and 20 DEGs were upregulated ( $1 < \log_2$  (fold change)  $< 4.7$ ). Several known regulatory genes of PPDE production, such as *PoxCxrB* [26], *PoxClrB* [32], *PoxRfxA* [33], *PoxPacC* [34], *POX01118* [35], *POX05276* [26], *POX09124*, and *POX09469* [36] were found, as well as *PoxBrlA* [37], *PoxFlbD*, and *PoxAbaA*—known to activate conidiation in filamentous fungi [38]. Moreover, 25 DEGs encoding sugar transporters were found by InterPro screening in  $\Delta PoxMKK1$ , such as *PoxCdtD* ( $\log_2$  (fold change) =  $-2.20$ ), *PoxCdtC* ( $\log_2$  (fold change) =  $-1.89$ ), and *PoxRCO-3* ( $\log_2$  (fold change) =  $-3.99$ ) (Figure 5D).

### 3.6. Regulation Kinetics of *PoxMKK1* on the Expression of Major Genes Encoding PPDE and TFs in *P. oxalicum* under SmF and SSF

In order to further validate the influences of *PoxMKK1* on major PPDE- and TF-encoding genes at the transcriptional level, RT-qPCR analysis was conducted on selected genes as shown in Figure 6. Deletion of *PoxMKK1* significantly reduced the expression of four genes (*cbh2*, *Cel5B*, *Bgl3A*, and *POX06079*) encoding major cellulase and two xylanase genes (*Xyn10A* and *Xyn11B*) in *P. oxalicum* under SmF and SSF by 9.12–99.68%, as compared with the control  $\Delta PoxKu70$  strain (Figure 6A). Notably, the transcriptional levels of amylase genes (*Amy15A*, *POX02412*, and *Amy13A*) in  $\Delta PoxMKK1$  were significantly higher than those in  $\Delta PoxKu70$  by 4.38- to 12.34-fold under 4 h of induction by SCS with SmF, whereas these decreased by 64.66–94.61% at later induction stages (Figure 6C).

Furthermore, under SmF with Avicel and SSF with WR, the transcriptional level of cellulase activator gene *PoxClrB* decreased by 27.95–63.45% and 31.23–67.22% in  $\Delta PoxMKK1$  compared with those in  $\Delta PoxKu70$ , respectively (Figure 6D). In contrast, the expression of *PoxBrlA* was increased 1.97–705.31 times in  $\Delta PoxMKK1$ , which is consistent with the RNA-seq data (Figure 6E). Under SmF with SCS, *PoxClrB* and *PoxAmyR* expression was markedly less in  $\Delta PoxMKK1$  than in  $\Delta PoxKu70$  (Figure 6F).

### 3.7. Comparative Analysis of *PoxMK1* and *PoxMKK1* Regulons in *P. oxalicum*

As previously described, *PoxMKK1* was an orthologue of *Ste7* in *S. cerevisiae*, which was located in upstream of the MAP kinase *Fus3/Kss1* in the mating/filamentation–invasion signaling pathway. Therefore, it was necessary to ascertain the overlapped regulons mediated by *PoxMKK1* and *PoxMK1* in *P. oxalicum*.

Comparative analysis suggested that there were 611 shared DEGs in the regulons of *PoxMKK1* and *PoxMK1*. Among them, the regulatory function of 590 co-regulated genes was consistent between  $\Delta PoxMKK1$  and  $\Delta PoxMK1$ , including 303 upregulated and 267 downregulated genes, compared with the control strain  $\Delta PoxKu70$  (Figure 7A,B). Interestingly, 7 cellulase genes (i.e., 1 *cbh*, 5 *egs*, and 1 *bgl*), 5 xylanase genes, 23 TF genes (e.g., *PoxCxrB*, *PoxClrB*, *PoxBrlA*, *PoxFlbD*, and *PoxAbaA*), and 16 putative sugar transporter genes (e.g., *PoxCdtD*, *PoxCdtC*, and *PoxRCO-3*) were found in the co-regulated DEGs set (Figure 7C–E), indicating that the  $\Delta PoxMK1$  and  $\Delta PoxMKK1$  mutants shared similar transcriptional profiles.



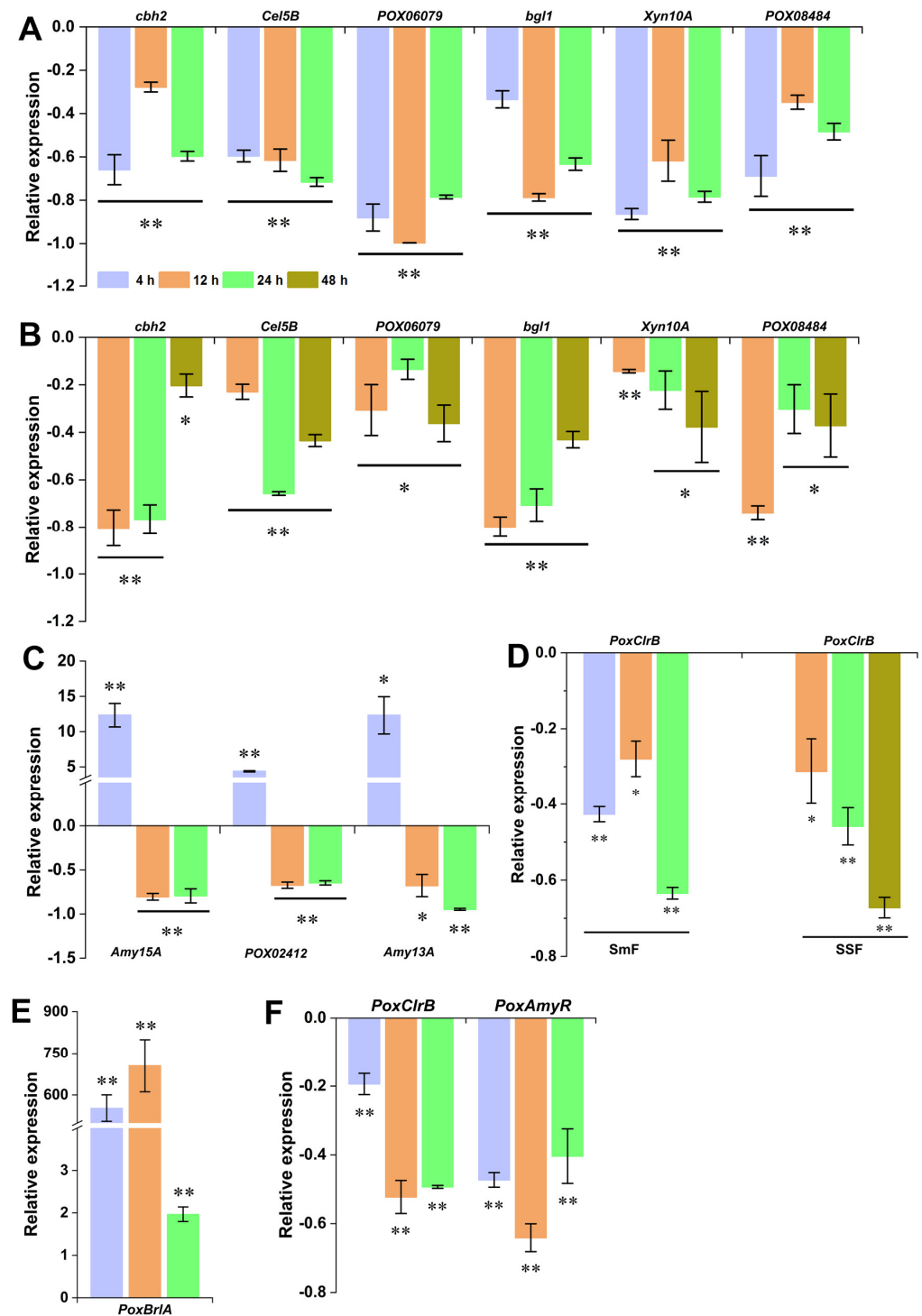


**Figure 6.** Key gene expression analysis of *P. oxalicum* strains by RT-qPCR assay. (A,B) Expression abundance of major cellulase and xylanase genes under SmF and SSF. (C) Expression abundance of major amylase genes. (D) Expression abundance of known transcription factor (TF) genes for regulating cellulase and xylanase production. (E) Expression abundance of known TF genes for regulating amylase production. (F) Expression abundance of *BrlA* gene involved in asexual development. The transcript levels of each gene were tested at three different times (at 4, 12, and 24 h under SmF and at 12, 24, and 48 h under SSF) after a transfer and were then standardized against those of the control strain  $\Delta PoxKu70$ . \*  $p < 0.05$  and \*\*  $p < 0.01$  according to Student's *t*-test indicated significant differences between the mutant  $\Delta PoxMKK1$  and the control strain.

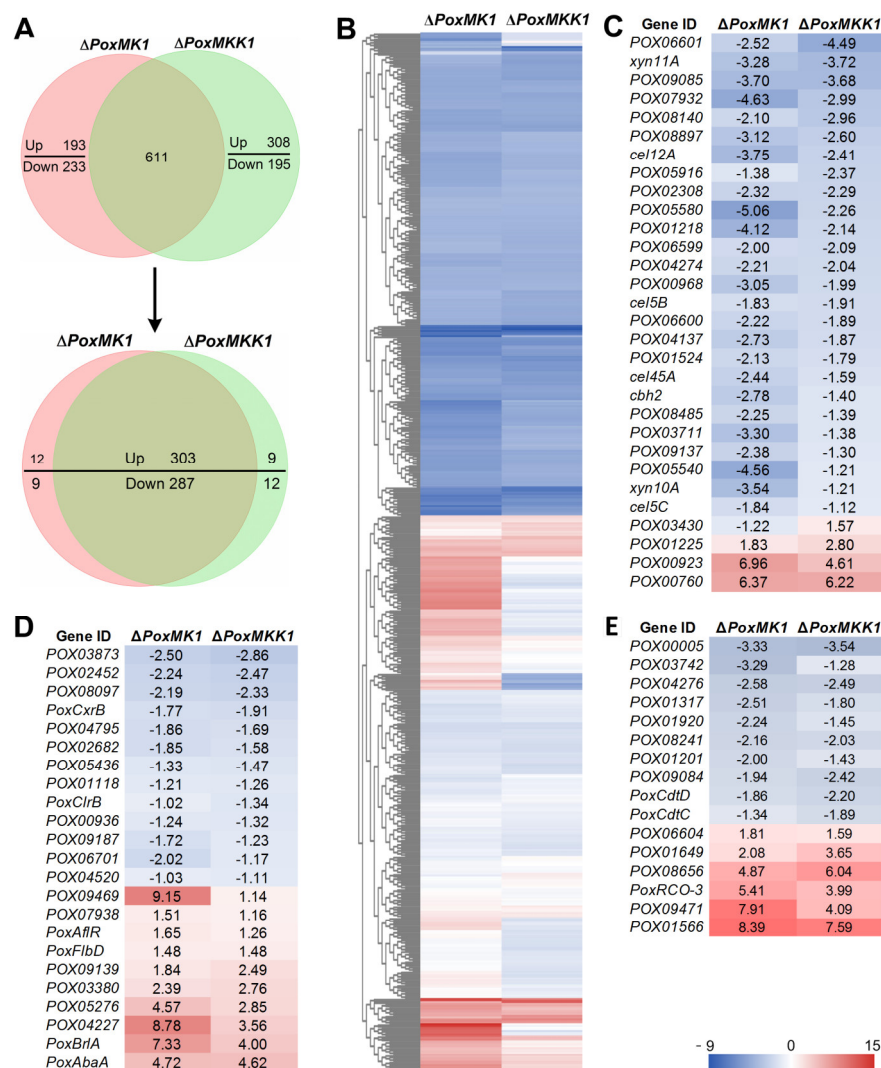


**Figure 7.** Regulon comparison of *PoxMK1* and *PoxMkk1* deduced by Avicel for 24 h. (A) Number of co-regulated differentially expressed genes (DEGs). (B) Heatmap illustrating co-regulated DEGs; (C–E) DEGs encoding predicted CAZymes, TFs, and sugar transporters.

#### 4. Discussion

As one of the multicellular eukaryotic organisms, the growth and development of filamentous fungi are regulated by evolutionarily conserved signal transduction pathways in which protein kinases are major players. In this study, the function of protein kinase *PoxMkk1*, a mediate component of three-tiered cascade kinases in the Fus3/Kss1-MAP kinase module, was investigated in *P. oxalicum* for the first time. *PoxMkk1* is involved in modulating the production of PPDE—including cellulase, xylanase, and amylase, under both SSF and SmF conditions—the regulation of vegetative growth and conidiation.

In previous studies, MAPK modules were found to be involved in the regulation of the production of PPDE in fungi. For instance, three MAPKs are identified as *Tmk1*, *Tmk2*, and *Tmk3* in *T. reesei*, which are homologous to yeast *Hog1*, *Slt2*, and *Fus3*, respectively [39]. Among of them, *Tmk3* promotes cellulase production, whereas *Tmk2* represses cellulase formation [40,41]. Deletion of gene *Tmk1* improves cellulase formation, but does not influence the expression of major cellulase genes [39]. However, when cultivated on sugarcane bagasse, the production of cellulase and xylanase by mutant  $\Delta tmk2$  decreases significantly by repressing the transcription of major PPDE-encoding genes [42]. The upstream components of the *Tmk3* signaling cascade, including *TrSho1*, *TrSte20*, and *TrYpd1*, differentially regulate cellulase production. Loss of *TrSte20* or repression of *TrSho1* significantly dimin-

ishes the transcriptional levels of cellulase genes, whereas overexpression of *TrYpd1* reduces the production of cellulase and repression of *TrYpd1* hardly affects cellulase induction [43]. In *A. nidulans*, xylanase activity is significantly reduced in the  $\Delta ste7$  and  $\Delta mpkB$  mutants, but it is significantly increased in the  $\Delta pbsA$  mutant induced by xylose and/or glucose, especially after 72 h [44]. In some plant pathogenic fungi, such as *F. graminearum* [45], *A. brassicicola* [46,47], and *Valsa mali* [48] MAPK pathways also play an important role in the secretion of PPDE.

In the current study, the regulation of protein kinase PoxMkk1 for PPDE production was characterized in *P. oxalicum*. Although PoxMkk1 mainly positively regulated the production of cellulase and xylanase, fine regulation was different between SmF and SSF conditions. For example, under SmF, pNPGase production of mutant  $\Delta PoxMkk1$  was significantly increased on day 2 after a transfer but was drastically decreased on day 4, while under SSF, pNPGase production remarkably reduced during the whole cultivation period compared with that of the control strain  $\Delta PoxKu70$ . These conditions might have resulted from the fermentation format. During SSF, enough moisture was present on the surface of the porous and moist solid substrate particles to contribute to the development of fungal hyphae. Compared with SmF, SSF improves the kinetic parameters associated with growth and fungal morphology, modifies the expression of many genes, prevents catabolite repression, and increases the secretome complexity, which mimics their natural habitat [49,50]. Previous work demonstrated different transcription profiles of *P. oxalicum* cultivated under SSF and SmF. For instance, major cellulase genes increased their transcripts under SSF in comparison with those under SmF, but genes participating in the citric acid cycle were down-regulated, hinting that a distinct regulatory network was exhibited in *P. oxalicum* under SSF and SmF [36]. However, uncovering the detailed mechanism of PoxMkk1 functions would require further study under SSF and SmF, respectively.

Additionally, the restorative effect of cellulase and xylanase production was observed to result from gene *PoxMkk1* deletion under SSF, which also occurred in *T. reesei*  $\Delta tmk3$  [41]. Accordingly, the effects of PoxMkk1 on PPDE production were dependent on carbon source, cultivation time and fermentation mode in *P. oxalicum*.

Moreover, it should be noted that the expression of major amylase genes including *amy15A*, *POX02412*, and *amy13A* was dynamically regulated by PoxMkk1; for instance, the expression of these genes was increased at 4 h of induction in the mutant  $\Delta PoxMkk1$  in comparison with the  $\Delta PoxKu70$ , whereas it was downregulated at 12 and 24 h. This result should be attributed to the induction of an extracellular complex carbon source. Starch consists of multiple glucose units that are linked by  $\alpha$ -1,4-glycosidic bonds and branched by  $\alpha$ -1,6-glycosidic bonds, which could be hydrolyzed by amylase. Amylase consists of four related enzymes,  $\alpha$ -amylase (EC 3.2.1.1), glucoamylase (EC 3.2.1.3),  $\alpha$ -glucosidase (EC 3.2.1.20), and 1,4- $\alpha$ -glucanbranching enzyme (EC 2.4.1.18).  $\alpha$ -amylase breaks  $\alpha$ -1,4-glycosidic bonds into amylopectin, or amylose straight chains, to release straight-chain and branched oligosaccharides of various lengths. Glucoamylase can cleave both  $\alpha$ -1,4- or  $\alpha$ -1,6-glycosidic bonds at the non-reducing ends of starch chains, or dextrans, to release glucose [51]. Filamentous fungi secrete a large number of starch-hydrolytic enzymes, all of which are induced by starch, dextrin, or maltose to different extents but depending on the requirement of fungal cells.

Furthermore, regulon comparative analysis showed that there was cross-talk regulation mediated by PoxMk1 and PoxMkk1 and that lots of DEGs, such as essential TF and sugar transporter genes, are co-regulated by them (Figure 8). ClrB is a crucial TF for cellulase activation in the presence of cellulose [52], while BrlA, as a central regulator of conidiation, not only plays an extensive role in the regulation of secondary metabolism, but also negatively regulates the expression of cellulase genes [37]. CxB is a C2H2-type zinc finger TF for positively regulating the production of cellulase and xylanase, which directly bound the promoter regions of *BrlA* [22,26]. The sugar transporters are important for the utilization of lignocellulose, and of them, cellodextrin transporters CdtC and CdtD are necessary for the induction of cellulase expression [53]. A non-transporting glucose

sensor, RCO-3, is involved in the regulation of the glucose transport system, and leads to carbon catabolite repression [54]. Additionally, direct interaction between PoxMK1 and POX06496/Hog1 was detected in Y2H assays. Deletion of gene *PoxMK1* enhances the phosphorylation of POX06496/Hog1, which phosphorylates PoxAtf1 to depress the expression of cellulase and xylanase genes [23]. These results reveal that PoxMK1 may regulate the production of cellulase and xylanase via PoxMK1.

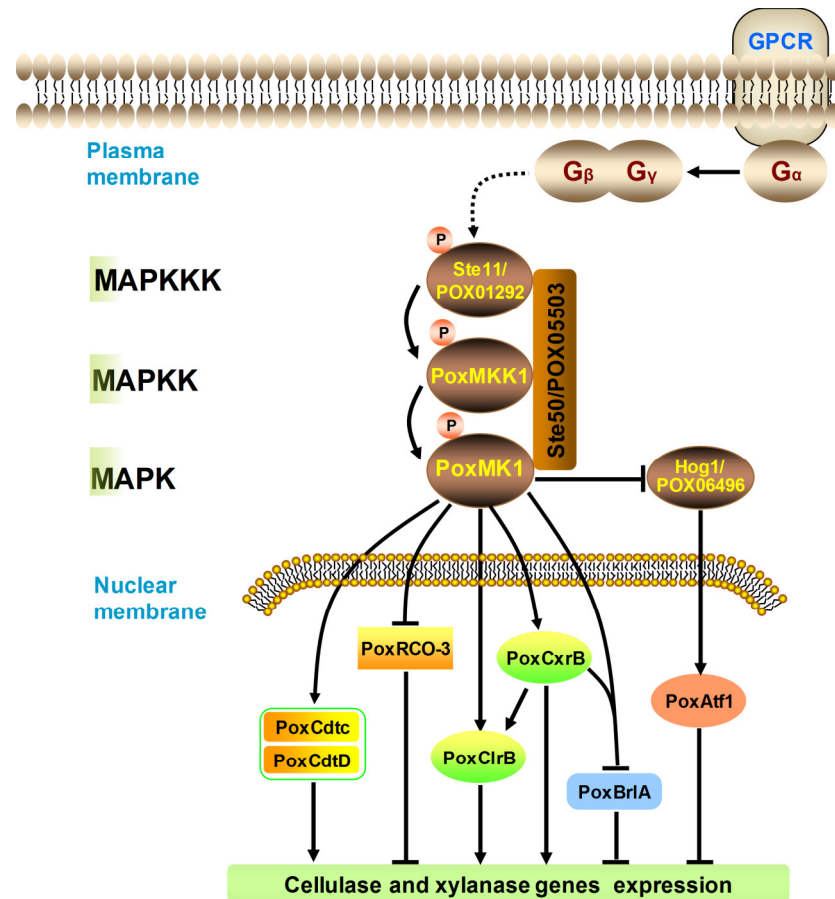


**Figure 8.** Schematic model for the regulatory network of protein kinase PoxMK1 in *P. oxalicum* according to the data. GPCRs, G protein-coupled receptor. A P in orange-red circles represents phosphorylation events. The dashed lines represent that the pathway needs to be further confirmed. Arrows indicate activation, whereas bars indicate repression.

In *S. cerevisiae*, the heterotrimeric G-protein is initially separated into the G $\alpha$  and G $\beta\gamma$  response to external signals. The G $\beta\gamma$  recruits the scaffold protein Ste5, and then the Ste5 assembles Ste11, Ste7, and Fus3/Kss1 [7]. The adaptor protein Ste50 also tethers Ste11, which contributes to the phosphorylation of Ste11. However, the orthologs of Ste5 do not exist in many filamentous fungi [10]. Therefore, it can be postulated that the Fus3/Kss1 signaling pathway regulates the cellulase and xylanase production in a tetrameric manner, but further research will need to be carried out in order to confirm this.

In addition, vegetative growth and sporulation are two fundamental processes in filamentous fungi. Previous studies showed that a lack of Fus3/Kss1-type MAPK cascade was correlated with a reduced hyphal growth rate and asexual sporulation in *Neurospora crassa* [55], *Aspergillus flavus* [56], *A. fumigatus* [57], *Aspergillus niger* [58], and *Botrytis cinerea* [59]. In *Cryphonectria parasitica*, although deletion of the gene *cpk2* results in impaired growth on PDA plates, the biomass weight was similar to that of the wild-type strain in CM [60]. In *Colletotrichum higginsianum*, the *ChSte7* disruption mutant shows extremely decreased growth on PDA, biomass accumulation in PDB, and conidial germination, but produces as many conidia as the wild-type strain [61]. In *Fusarium graminearum*, the mutant



$\Delta FgSte7$  grows obviously more slowly than the wild-type progenitor on the plates of PDA, CM, and minimum medium, and exhibits a significant decrease in conidiation after 4 days of incubation [45]. In *B. bassiana*, mutant  $\Delta mkk6$  showed much less-severe growth defects on rich SDAY plates than on minimal CZA plates with different carbon or nitrogen sources, and the conidial yield was reduced by 78% on SDAY plates [14]. However, our study found that the mutant  $\Delta PoxMKK1$  grew faster than the control strain on PDA plates, though it showed no significant difference on the plates of MMM with glucose, SCS, or Avicel. Moreover, the dry mycelium weight of  $\Delta PoxMKK1$  in MMM with either glucose or Avicel showed a visible decrease compared to that of  $\Delta PoxKu70$ , while no difference was displayed in CM and MMM with SCS. Interestingly, the asexual spores of the  $\Delta PoxMKK1$  were reduced significantly on the above-mentioned solid plates, but they increased significantly in the liquid media. When cultivated for 2 days under SmF, phialides differentiated from the hypha tip of the  $\Delta PoxMKK1$ . Furthermore, the transcriptions of conidiation-activator genes *FlbD*, *BrlA*, and *AbaA* in the  $\Delta PoxMKK1$  increased by several to dozens of folds compared with those in the control strain under SmF, deduced by Avicel for 24 h after a shift. As is known, the TF *BrlA* is essential and sufficient for conidiation in filamentous fungi, and it is activated by *FlbD* and *AbaA*, and the *AbaA* is required for the differentiation of phialides [38], which suggests that spore production and hypha differentiation are consistent with the expression of conidiation-related TF genes in  $\Delta PoxMKK1$  under SmF. Consequently, the *Ste7* homologue *PoxMKK1* affects vegetative growth and conidiation, which is not only related to species, but also to cultural conditions in filamentous fungi.

In future studies, we should investigate the influence of the simultaneous manipulation of gene *PoxMKK1* with other regulatory genes by, for example, constructing double/triple gene-deleted/overexpressed mutant, with the aim of maximizing PPDE production, which can potentially assist with the saccharification of lignocellulosic biomass. In addition, the heterologous expression of gene *PoxMKK1* in other systems such as *Trichoderma reesei* should be considered in order to possibly minimize the regulatory side-effects of its expression. Alternatively, the expression of gene *PoxMKK1* could be fine-tuned via the manipulation of promoter and terminator in *P. oxalicum* in order to improve PPDE production.

In summary, our study reveals that the protein kinase *PoxMKK1* modulated PPDE production, vegetative growth, and asexual sporogenesis in *P. oxalicum*. The functional characterization of *PoxMKK1* will contribute to our understanding of the molecular mechanisms involved in morphogenesis and the regulation of processes of cellulolytic enzyme synthesis by the *Fus3/Kss1* signaling pathway. In turn, this may allow for the development of strategies to construct an engineering strain with high PPDE production by rational design.

**Supplementary Materials:** The following supporting information can be downloaded at: <https://www.mdpi.com/article/10.3390/jof9040397/s1>, Figure S1: Screening of *PoxMK1*-interacting protein in *P. oxalicum* using yeast two hybrid approach; Figure S2: Deletion mutants confirmation of *PoxMK1*-interacting protein gene in *P. oxalicum*; Figure S3: FPase production of the control strain  $\Delta PoxKu70$  and mutants  $\Delta POX04853$ ,  $\Delta POX06496$ ,  $\Delta POX07588$  and  $\Delta POX07948$ ; Figure S4: PCR verification of complementary strain *CPoxMKK1*; Figure S5: Biomass determination of *P. oxalicum* mutant  $\Delta PoxMKK1$  and the control strain  $\Delta PoxKu70$  in different liquid medium at 28 °C with 180 rpm for 72 h; Figure S6: Conidia number of *P. oxalicum* mutant  $\Delta PoxMKK1$ , complementation strain *CPoxMKK1* and the control strain  $\Delta PoxKu70$ ; Figure S7: Pearson's correlation analysis of the transcriptomes of *P. oxalicum* mutant strain  $\Delta PoxMKK1$  and the control strain  $\Delta PoxKu70$ ; Table S1: Primers used in this study; Table S2: List of 1114 differentially expressed genes in *P. oxalicum* mutant  $\Delta PoxMKK1$  compared with the control strain  $\Delta PoxKu70$  in the presence of Avicel.

**Author Contributions:** Both S.Z. and J.-X.F. contributed to the conception, study design, supervision, and manuscript writing—review and editing. B.M. was responsible for investigation, data acquisition, statistical analysis, visualization, and original draft preparation. X.-M.L. was responsible for the literature search, experimental preparation, and partial data collection. All authors have read and agreed to the published version of the manuscript.

**Funding:** This research was funded by the National Natural Science Foundation of China (U21A20178) and the Key Research and Development Program Project of Guangxi (Guike AB21076010).

**Institutional Review Board Statement:** Not applicable.

**Informed Consent Statement:** Not applicable.

**Data Availability Statement:** All data are available in the article.

**Conflicts of Interest:** The authors have no conflict of interest to declare.

## References

1. De Vries, R.P.; Mäkelä, M.R. Genomic and Postgenomic Diversity of Fungal Plant Biomass Degradation Approaches. *Trends Microbiol.* **2020**, *6*, 487–499. [[CrossRef](#)]
2. Francois, J.M.; Alkim, C.; Morin, N. Engineering Microbial Pathways for Production of Bio-Based Chemicals from Lignocellulosic Sugars: Current Status and Perspectives. *Biotechnol. Biofuels* **2020**, *13*, 118. [[CrossRef](#)]
3. Bryant, N.D.; Pu, Y.Q.; Tschaplinski, T.J.; Tuskan, G.A.; Muchero, W.; Kalluri, U.C.; Yoo, C.G.; Ragauskas, A.J. Transgenic Poplar Designed for Biofuels. *Trends Plant Sci.* **2020**, *9*, 881–896. [[CrossRef](#)] [[PubMed](#)]
4. Benocci, T.; Aguilar-Pontes, M.V.; Zhou, M.M.; Seiboth, B.; de Vries, R.P. Regulators of Plant Biomass Degradation in Ascomycetous Fungi. *Biotechnol. Biofuels* **2017**, *10*, 152. [[CrossRef](#)] [[PubMed](#)]
5. Lin, L.C.; Wang, S.S.; Li, X.L.; He, Q.; Benz, J.P.; Tian, C.G. STK-12 Acts as a Transcriptional Brake to Control the Expression of Cellulase-Encoding Genes in *Neurospora crassa*. *PLoS Genet.* **2019**, *11*, e1008510. [[CrossRef](#)]
6. Rodriguez-Iglesias, A.; Schmoll, M. Protein Phosphatases Regulate Growth, Development, Cellulases and Secondary Metabolism in *Trichoderma reesei*. *Sci. Rep.* **2019**, *1*, 10995. [[CrossRef](#)]
7. Martínez-Soto, D.; Ruiz-Herrera, J. Functional Analysis of the MAPK Pathways in Fungi. *Rev. Iberoam. Micol.* **2017**, *4*, 192–202. [[CrossRef](#)] [[PubMed](#)]
8. González-Rubio, G.; Fernández-Acero, T.; Martín, H.; Molina, M. Mitogen-Activated Protein Kinase Phosphatases (Mkps) in Fungal Signaling: Conservation, Function, and Regulation. *Int. J. Mol. Sci.* **2019**, *7*, 1709. [[CrossRef](#)]
9. Tong, S.M.; Feng, M.G. Insights into Regulatory Roles of MAPK-Cascaded Pathways in Multiple Stress Responses and Life Cycles of Insect and Nematode Mycopathogens. *Appl. Microbiol. Biotechnol.* **2019**, *2*, 577–587. [[CrossRef](#)]
10. Frawley, D.; Bayram, Ö. The Pheromone Response Module, a Mitogen-Activated Protein Kinase Pathway Implicated in the Regulation of Fungal Development, Secondary Metabolism and Pathogenicity. *Fungal. Genet. Biol.* **2020**, *144*, 103469. [[CrossRef](#)]
11. Izumitsu, K.; Yoshimi, A.; Kubo, D.; Morita, A.; Saitoh, Y.; Tanaka, C. The MAPKK Kinase Chste11 Regulates Sexual/Asexual Development, Melanization, Pathogenicity, and Adaptation to Oxidative Stress in *Cochliobolus heterostrophus*. *Curr. Genet.* **2009**, *4*, 439–448. [[CrossRef](#)]
12. Wasserstrom, L.; Lengeler, K.B.; Walther, A.; Wendland, J. Molecular Determinants of Sporulation in *Ashbya gossypii*. *Genetics* **2013**, *1*, 87–99. [[CrossRef](#)]
13. Xu, H.J.; Zhang, Q.Q.; Cui, W.J.; Zhang, X.F.; Liu, W.Y.; Zhang, L.; Islam, M.N.; Baek, K.H.; Wang, Y.J. *AbSte7*, a MAPKK Gene of *Alternaria brassicicola*, is Involved in Conidiation, Salt/Oxidative Stress, and Pathogenicity. *J. Microbiol. Biotechnol.* **2016**, *7*, 1311–1319. [[CrossRef](#)] [[PubMed](#)]
14. Liu, J.; Sun, H.H.; Ying, S.H.; Feng, M.G. Characterization of Three Mitogen-Activated Protein Kinase Kinase-Like Proteins in *Beauveria bassiana*. *Fungal. Genet. Biol.* **2018**, *113*, 24–31. [[CrossRef](#)]
15. Zhang, Y.F.; Ge, Q.W.; Cao, Q.C.; Cui, H.F.; Hu, P.; Yu, X.P.; Ye, Z.H. Cloning and Characterization of Two MAPK Genes UeKpp2 and UeKpp6 in *Ustilago esculenta*. *Curr. Microbiol.* **2018**, *8*, 1016–1024. [[CrossRef](#)]
16. Yu, L.; Xiong, D.G.; Han, Z.; Liang, Y.M.; Tian, C.G. The Mitogen-Activated Protein Kinase Gene CcPmk1 is Required for Fungal Growth, Cell Wall Integrity and Pathogenicity in *Cytospora chrysosperma*. *Fungal. Genet. Biol.* **2019**, *128*, 1–13. [[CrossRef](#)]
17. Wang, X.L.; Lu, D.X.; Tian, C.M. Mitogen-Activated Protein Kinase Cascade Cgste50-Ste11-Ste7-Mk1 Regulates Infection-Related Morphogenesis in the Poplar Anthracnose Fungus *Colletotrichum gloeosporioides*. *Microbiol. Res.* **2021**, *248*, 126748. [[CrossRef](#)] [[PubMed](#)]
18. Jiang, Y.F.; Qin, X.F.; Zhu, F.; Zhang, Y.F.; Zhang, X.C.; Hartley, W.; Xue, S.G. Halving Gypsum Dose by *Penicillium oxalicum* on Alkaline Neutralization and Microbial Community Reconstruction in Bauxite Residue. *Chem. Eng. J.* **2023**, *451*, 139008. [[CrossRef](#)]
19. Hao, S.F.; Wang, P.Y.; Ge, F.; Li, F.; Deng, S.Q.; Zhang, D.Y.; Tian, J. Enhanced Lead (Pb) Immobilization in Red Soil by Phosphate Solubilizing Fungi Associated with Tricalcium Phosphate Influencing Microbial Community Composition and Pb Translocation in *Lactuca sativa* L. *J. Hazard Mater.* **2022**, *424*, 127720. [[CrossRef](#)]
20. Li, C.X.; Liu, L.; Zhang, T.; Luo, X.M.; Feng, J.X.; Zhao, S. Three-Dimensional Genome Map of the Filamentous Fungus *Penicillium oxalicum*. *Microbiol. Spectr.* **2022**, *3*, e0212121. [[CrossRef](#)] [[PubMed](#)]
21. Hu, Y.B.; Liu, G.D.; Li, Z.H.; Qin, Y.Q.; Qu, Y.B.; Song, X. G Protein-cAMP Signaling Pathway Mediated by PGA3 Plays Different Roles in Regulating the Expressions of Amylases and Cellulases in *Penicillium decumbens*. *Fungal Genet. Biol.* **2013**, *58–59*, 62–70. [[CrossRef](#)] [[PubMed](#)]

22. Pang, X.M.; Tian, D.; Zhang, T.; Liao, L.S.; Li, C.X.; Luo, X.M.; Feng, J.X.; Zhao, S. G Protein  $\gamma$  Subunit Modulates Expression of Plant-Biomass-Degrading Enzyme Genes and Mycelial-Development-Related Genes in *Penicillium oxalicum*. *Appl. Microbiol. Biotechnol.* **2021**, *11*, 4675–4691. [[CrossRef](#)] [[PubMed](#)]
23. Ma, B.; Ning, Y.N.; Li, C.X.; Tian, D.; Guo, H.; Pang, X.M.; Luo, X.M.; Zhao, S.; Feng, J.X. A Mitogen-Activated Protein Kinase PoxMK1 Mediates Regulation of the Production of Plant-Biomass-Degrading Enzymes, Vegetative growth, and Pigment Biosynthesis in *Penicillium oxalicum*. *Appl. Microbiol. Biotechnol.* **2021**, *2*, 661–678. [[CrossRef](#)] [[PubMed](#)]
24. Zhao, S.; Yan, Y.S.; He, Q.P.; Yang, L.; Yin, X.; Li, C.X.; Mao, L.C.; Liao, L.S.; Huang, J.Q.; Xie, S.B.; et al. Comparative Genomic, Transcriptomic and Secretomic Profiling of *Penicillium oxalicum* HP7-1 and its Cellulase and Xylanase Hyper-Producing Mutant EU2106, and Identification of Two Novel Regulatory Genes of Cellulase and Xylanase Gene Expression. *Biotechnol. Biofuels* **2016**, *9*, 203. [[CrossRef](#)] [[PubMed](#)]
25. Zhang, T.; Mai, R.M.; Fang, Q.Q.; Ou, J.F.; Mo, L.X.; Tian, D.; Li, C.X.; Gu, L.S.; Luo, X.M.; Feng, J.X.; et al. Regulatory function of the Novel Transcription Factor CxrC in *Penicillium oxalicum*. *Mol. Microbiol.* **2021**, *6*, 1512–1532. [[CrossRef](#)]
26. Yan, Y.S.; Zhao, S.; Liao, L.S.; He, Q.P.; Xiong, Y.R.; Wang, L.; Li, C.X.; Feng, J.X. Transcriptomic Profiling and Genetic Analyses Reveal Novel Key Regulators of Cellulase and Xylanase Gene Expression in *Penicillium oxalicum*. *Biotechnol. Biofuels* **2017**, *1*, 279. [[CrossRef](#)]
27. Götz, S.; García-Gómez, J.M.; Terol, J.; Williams, T.D.; Nagaraj, S.H.; Nueda, M.J.; Robles, M.; Talón, M.; Dopazo, J.; Conesa, A. High-Throughput Functional Annotation and Data Mining with the Blast2GO suite. *Nucleic Acids Res.* **2008**, *10*, 3420–3435. [[CrossRef](#)]
28. Livak, K.J.; Schmittgen, T.D. Analysis of Relative Gene Expression Data Using Real-Time Quantitative PCR and the 2<sup>-Delta Delta</sup> C(T) Method. *Methods* **2001**, *4*, 402–408. [[CrossRef](#)]
29. Su, L.H.; Zhao, S.; Jiang, S.X.; Liao, X.Z.; Duan, C.J.; Feng, J.X. Cellulase with High  $\beta$ -Glucosidase Activity by *Penicillium oxalicum* Under Solid State Fermentation and Its Use in Hydrolysis of Cassava Residue. *World J. Microbiol. Biotechnol.* **2017**, *2*, 37. [[CrossRef](#)]
30. Larkin, M.A.; Blackshields, G.; Brown, N.P.; Chenna, R.; McGettigan, P.A.; McWilliam, H.; Valentin, F.; Wallace, I.M.; Wilm, A.; Lopez, R.; et al. Clustal W and Clustal X version 2.0. *Bioinformatics* **2007**, *21*, 2947–2948. [[CrossRef](#)]
31. Kumar, S.; Stecher, G.; Li, M.; Nknyaz, C.; Tamura, K. MEGA X: Molecular Evolutionary Genetics Analysis Across Computing Platforms. *Mol. Biol. Evol.* **2018**, *6*, 1547–1549. [[CrossRef](#)]
32. Li, Z.H.; Yao, G.S.; Wu, R.M.; Gao, L.W.; Kan, Q.B.; Liu, M.; Yang, P.; Liu, G.D.; Qin, Y.Q.; Song, X.; et al. Synergistic and Dose-Controlled Regulation of Cellulase Gene Expression in *Penicillium oxalicum*. *PLoS Genet.* **2015**, *9*, e1005509. [[CrossRef](#)] [[PubMed](#)]
33. Liao, G.Y.; Zhao, S.; Zhang, T.; Li, C.X.; Liao, L.S.; Zhang, F.F.; Luo, X.M.; Feng, J.X. The Transcription Factor TpRfx1 is an Essential Regulator of Amylase and Cellulase Gene Expression in *Talaromyces pinophilus*. *Biotechnol. Biofuels* **2018**, *11*, 276. [[CrossRef](#)] [[PubMed](#)]
34. Kunitake, E.; Hagiwara, D.; Miyamoto, K.; Kanamaru, K.; Kimura, M.; Kobayashi, T. Regulation of Genes Encoding Cellulolytic Enzymes by Pal-PacC Signaling in *Aspergillus nidulans*. *Appl. Microbiol. Biotechnol.* **2016**, *8*, 3621–3635. [[CrossRef](#)] [[PubMed](#)]
35. Li, C.X.; Zhao, S.; Luo, X.M.; Feng, J.X. Weighted Gene Co-Expression Network Analysis Identifies Critical Genes for the Production of Cellulase and Xylanase in *Penicillium oxalicum*. *Front. Microbiol.* **2020**, *11*, 520. [[CrossRef](#)]
36. Zhao, S.; Liu, Q.; Wang, J.X.; Liao, X.Z.; Guo, H.; Li, C.X.; Zhang, F.F.; Liao, L.S.; Luo, X.M.; Feng, J.X. Differential Transcriptomic Profiling of Filamentous Fungus During Solid-State and Submerged Fermentation and Identification of an Essential Regulatory Gene PoxMBF1 that Directly Regulated Cellulase and Xylanase Gene Expression. *Biotechnol. Biofuels* **2019**, *12*, 103. [[CrossRef](#)]
37. Qin, Y.Q.; Bao, L.F.; Gao, M.R.; Chen, M.; Lei, Y.F.; Liu, G.D.; Qu, Y.B. *Penicillium decumbens* BrlA Extensively Regulates Secondary Metabolism and Functionally Associates with the Expression of Cellulase Genes. *Appl. Microbiol. Biotechnol.* **2013**, *24*, 10453–10467. [[CrossRef](#)]
38. Park, H.S.; Yu, J.H. Genetic Control of Asexual Sporulation in Filamentous Fungi. *Curr. Opin. Microbiol.* **2012**, *6*, 669–677. [[CrossRef](#)]
39. Wang, M.Y.; Zhang, M.L.; Li, L.; Dong, Y.M.; Jiang, Y.; Liu, K.M.; Zhang, R.Q.; Jiang, B.J.; Niu, K.L.; Fang, X. Role of *Trichoderma reesei* Mitogen-Activated Protein Kinases (MAPKs) in Cellulase Formation. *Biotechnol. Biofuels* **2017**, *10*, 99. [[CrossRef](#)]
40. Wang, M.Y.; Dong, Y.M.; Zhao, Q.S.; Wang, F.Z.; Liu, K.M.; Jiang, B.J.; Fang, X. Identification of the Role of a MAP kinase Tmk2 in *Hypocrea jecorina* (*Trichoderma reesei*). *Sci. Rep.* **2014**, *4*, 6732. [[CrossRef](#)] [[PubMed](#)]
41. Wang, M.Y.; Zhao, Q.S.; Yang, J.; Jiang, B.J.; Wang, F.Z.; Liu, K.M.; Fang, X. A Mitogen-Activated Protein Kinase Tmk3 Participates in High Osmolarity Resistance, Cell Wall Integrity Maintenance and Cellulase Production Regulation in *Trichoderma reesei*. *PLoS ONE* **2013**, *8*, e72189. [[CrossRef](#)]
42. de Paula, R.G.; Antoniôto, A.C.C.; Carraro, C.B.; Lopes, D.C.B.; Persinoti, G.F.; Peres, N.T.A.; Martinez-Rossi, N.M.; Silva-Rocha, R.; Silva, R.N. The Duality of the MAPK Signaling Pathway in the Control of Metabolic Processes and Cellulase Production in *Trichoderma reesei*. *Sci. Rep.* **2018**, *1*, 14931. [[CrossRef](#)]
43. Wang, Z.X.; An, N.; Xu, W.; Zhang, W.Q.; Meng, X.F.; Chen, G.J.; Liu, W.F. Functional Characterization of the Upstream Components of the Hog1-Like Kinase Cascade in Hyperosmotic and Carbon Sensing in *Trichoderma reesei*. *Biotechnol. Biofuels* **2018**, *1*, 97. [[CrossRef](#)] [[PubMed](#)]

44. de Assis, L.J.; Silva, L.P.; Liu, L.; Schmitt, K.; Valerius, O.; Braus, G.H.; Ries, L.N.A.; Goldman, G.H. The High Osmolarity Glycerol Mitogen-Activated Protein Kinase Regulates Glucose Catabolite Repression in Filamentous Fungi. *PLoS Genet.* **2020**, *8*, e1008996. [[CrossRef](#)]
45. Gu, Q.; Chen, Y.; Liu, Y.; Zhang, C.Q.; Ma, Z.H. The Transmembrane Protein FgSho1 Regulates Fungal Development and Pathogenicity via the MAPK Module Ste50-Ste11-Ste7 in *Fusarium graminearum*. *New Phytol.* **2015**, *1*, 315–328. [[CrossRef](#)]
46. Lu, K.; Zhang, M.; Yang, R.; Zhang, M.; Guo, Q.; Baek, K.H.; Xu, H.J. The MAP Kinase Kinase Gene *AbSte7* Regulates Multiple Aspects of *Alternaria brassicicola* Pathogenesis. *Plant Pathol. J.* **2019**, *2*, 91–99. [[CrossRef](#)]
47. Cho, Y.; Cramer, R.A., Jr.; Kim, K.H.; Davis, J.; Mitchell, T.K.; Figuli, P.; Pryor, B.M.; Lemasters, E.; Lawrence, C.B. The Fus3/Kss1 MAP Kinase Homolog Amk1 Regulates the Expression of Genes Encoding Hydrolytic Enzymes in *Alternaria brassicicola*. *Fungal Genet. Biol.* **2007**, *6*, 543–553. [[CrossRef](#)] [[PubMed](#)]
48. Wu, Y.X.; Xu, L.S.; Liu, J.; Yin, Z.Y.; Gao, X.N.; Feng, H.; Huang, L.L. A Mitogen-Activated Protein Kinase Gene (*VmPmk1*) Regulates Virulence and Cell Wall Degrading Enzyme Expression in *Valsa mali*. *Microb. Pathog.* **2017**, *111*, 298–306. [[CrossRef](#)]
49. Diaz, A.B.; Blandino, A.; Webb, C.; Caro, I. Modelling of Different Enzyme Productions by Solid-State Fermentation on Several Agro-Industrial Residues. *Appl. Microbiol. Biotechnol.* **2016**, *22*, 9555–9566. [[CrossRef](#)]
50. Salgado-Bautista, D.; Volke-Sepúlveda, T.; Figueroa-Martínez, F.; Carrasco-Navarro, U.; Chagolla-López, A.; Favela-Torres, E. Solid-State Fermentation Increases Secretome Complexity in *Aspergillus brasiliensis*. *Fungal Biol.* **2020**, *8*, 723–734. [[CrossRef](#)] [[PubMed](#)]
51. Wang, B.T.; Hu, S.; Yu, X.Y.; Jin, L.; Zhu, Y.J.; Jin, F.J. Studies of Cellulose and Starch Utilization and the Regulatory Mechanisms of Related Enzymes in Fungi. *Polymers* **2020**, *3*, 530. [[CrossRef](#)]
52. Kunitake, E.; Kobayashi, T. Conservation and Diversity of the Regulators of Cellulolytic Enzyme Genes in Ascomycete Fungi. *Curr. Genet.* **2017**, *6*, 951–958. [[CrossRef](#)] [[PubMed](#)]
53. Li, J.; Liu, G.; Chen, M.; Li, Z.; Qin, Y.; Qu, Y. Cellodextrin Transporters Play Important Roles in Cellulase Induction in the Cellulolytic Fungus *Penicillium oxalicum*. *Appl. Microbiol. Biotechnol.* **2013**, *24*, 10479–10488. [[CrossRef](#)]
54. Li, J.Y.; Liu, Q.; Li, J.G.; Lin, L.C.; Li, X.L.; Zhang, Y.L.; Tian, C.G. RCO-3 and COL-26 Form an External-to-Internal Module That Regulates the Dual-Affinity Glucose Transport System in *Neurospora crassa*. *Biotechnol. Biofuels* **2021**, *1*, 33. [[CrossRef](#)] [[PubMed](#)]
55. Maerz, S.; Ziv, C.; Vogt, N.; Helmstaedt, K.; Cohen, N.; Gorovits, R.; Yarden, O.; Seiler, S. The Nuclear Dbf2-Related Kinase COT1 and the Mitogen-Activated Protein Kinases MAK1 and MAK2 Genetically Interact to Regulate Filamentous Growth, Hyphal Fusion and Sexual Development in *Neurospora crassa*. *Genetics* **2008**, *3*, 1313–1325. [[CrossRef](#)]
56. Frawley, D.; Greco, C.; Oakley, B.; Alhussain, M.M.; Fleming, A.B.; Keller, N.P.; Bayram, Ö. The Tetrameric Pheromone Module SteC-MkkB-MpkB-SteD Regulates Asexual Sporulation, Sclerotia Formation and Aflatoxin Production in *Aspergillus flavus*. *Cell. Microbiol.* **2020**, *6*, e13192. [[CrossRef](#)]
57. Frawley, D.; Stroe, M.C.; Oakley, B.R.; Heinekamp, T.; Strassburger, M.; Fleming, A.B.; Brakhage, A.A.; Bayram, O. The Pheromone Module SteC-MkkB-MpkB-SteD-HamE Regulates Development, Stress Responses and Secondary Metabolism in *Aspergillus fumigatus*. *Front. Microbiol.* **2020**, *11*, 811. [[CrossRef](#)] [[PubMed](#)]
58. Priegnitz, B.E.; Brandt, U.; Pahirulzaman, K.A.; Dickschat, J.S.; Fleissner, A. The AngFus3 Mitogen-Activated Protein Kinase Controls Hyphal Differentiation and Secondary Metabolism in *Aspergillus niger*. *Eukaryot. Cell* **2015**, *6*, 602–615. [[CrossRef](#)]
59. Chamber, A.; Leroch, M.; Diwo, J.; Mendgen, K.; Hahn, M. The Role of Mitogen-Activated Protein (MAP) Kinase Signalling Components and the Ste12 Transcription Factor in Germination and Pathogenicity of *Botrytis cinerea*. *Mol. Plant Pathol.* **2010**, *1*, 105–119. [[CrossRef](#)]
60. Moretti, M.; Rossi, M.; Ciuffo, M.; Turina, M. Functional Characterization of the Three Mitogen-Activated Protein Kinase Kinases (MAP2Ks) Present in the *Cryphonectria parasitica* genome Reveals the Necessity of Cpkk1 and Cpkk2, but not Cpkk3, for Pathogenesis on Chestnut (*Castanea* spp.). *Mol. Plant Pathol.* **2014**, *5*, 500–512. [[CrossRef](#)]
61. Yuan, Q.F.; Chen, M.J.; Yan, Y.Q.; Gu, Q.N.; Huang, J.B.; Zheng, L. ChSte7 is Required for Vegetative Growth and Various Plant Infection Processes in *Colletotrichum higginsianum*. *Biomed. Res. Int.* **2016**, *2016*, 7496569. [[CrossRef](#)] [[PubMed](#)]

**Disclaimer/Publisher's Note:** The statements, opinions and data contained in all publications are solely those of the individual author(s) and contributor(s) and not of MDPI and/or the editor(s). MDPI and/or the editor(s) disclaim responsibility for any injury to people or property resulting from any ideas, methods, instructions or products referred to in the content.